Inorganic Chemistry

pubs.acs.org/IC Article

Tetra-Mn^{III}-Containing 30-Tungsto-4-phosphate, $[Mn^{III}_4(H_2O)_2(P_2W_{15}O_{56})_2]^{12-}$: Synthesis, Structure, XPS, Magnetism, and Electrochemical Study

Joydeb Goura, Manjiri Choudhari, Talha Nisar, Torsten Balster, Jasleen K. Bindra, Jared Kinyon, Bushra Ali, Timothy McCormac, Naresh S. Dalal, Veit Wagner, and Ulrich Kortz*

Cite This: *Inorg. Chem.* 2020, 59, 13034−13041 Read Online

ACCESS | Metrics & More | Article Recommendations | Supporting Information

ABSTRACT: Reaction of the mixed-valent Mn_{12}-acetato complex $[Mn^{III}_8Mn^{IV}_4O_{12}(CH_3COO)_{16}(H_2O)_4]$ with the trilacunary Wells-Dawson-type heteropolytungstate $[P_2W_{15}O_{56}]^{12-}$ in acidic acetate solution (pH 1.1) resulted in the tetra-Mn^{III}-containing polyanion $[Mn^{III}_4(H_2O)_2(P_2W_{15}O_{56})_2]^{12-}$ (**1**). Single-crystal XRD on $Na_{12}[Mn^{III}_4(H_2O)_2(P_2W_{15}O_{56})_2]\cdot 84H_2O$ (**1a**) revealed that four Mn^{III} ions form a rhombic Mn_4O_{16} core encapsulated by two $[P_2W_{15}O_{56}]^{12-}$ units. X-ray photoelectron spectroscopy (XPS) data confirm the +3 oxidation state of the four manganese ions in **1**. Magnetic measurements from 1.8−300 K in a 100 Oe magnetic field allowed for the extraction of full fitting parameters from the susceptibility data for **1**. The negative J_a value ($J_a = -2.16 \pm 0.08$ K, $J_b = 3.24 \pm 1.73$ K, $g = 2.35 \pm 0.040$, and $\rho = 0.34 \pm 0.03$) suggests a dominant antiferromagnetic spin exchange interaction between the four Mn^{III} ions, with the positive J_b being an accompanying result of J_a. Electrochemical studies revealed a reversible Mn^{IV}/Mn^{III} redox couple in **1** at the +0.80 to +1.1 V potential region with $E_{1/2} = +0.907$ V.

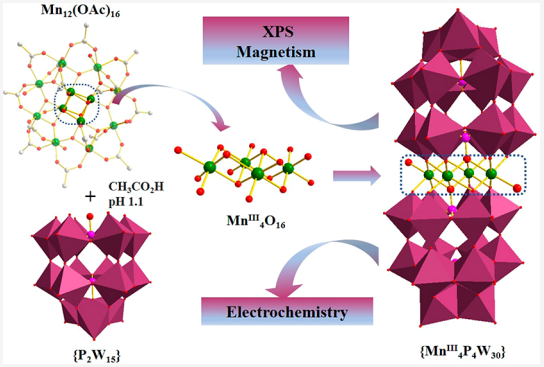

INTRODUCTION

Polyfunctional organic ligands have been widely used for the isolation of multinuclear 3d, 4f, and mixed 3d/4f metal-based coordination complexes.[1] Besides using such organic ligands, another class of inorganic multidentate ligands known as polyoxometalates (POMs) can be used to encapsulate multinuclear metal-oxo clusters. POMs are discrete, anionic metal oxides of early d-block metal ions (e.g., W^{VI}, Mo^{VI}, V^V) comprising edge- and corner-shared MO_6 octahedra which are usually synthesized in aqueous solution.[2] The most common examples of POMs are the Keggin (e.g., $SiW_{12}O_{40}^{4-}$) and the Wells-Dawson ions (e.g., $P_2W_{18}O_{62}^{6-}$). Lacunary (vacant) derivatives such as $SiW_{11}O_{39}^{8-}$, $P_2W_{17}O_{61}^{10-}$, and $P_2W_{15}O_{56}^{12-}$ are polydentate oxo-donors and hence highly reactive with d- and f-block metal ions.[3] Such behavior of lacunary POM ligands has resulted in a large number of compounds for various incorporated metal ion guests.[3,4] Among these, the encapsulation of magnetic metal ions in POMs is an interesting research area due to potential applications in molecular magnetism.[5] Our group has been active in the synthesis of magnetic POMs for many years, and some highlight examples include Cu^{II}_{20},[6a] Fe^{III}_{16},[6b] Co^{II}_{16},[6c,d] Ce^{III}_{20},[6e] and Dy^{III}_{12}[6f] containing heteropolytungstates. As concerns manganese, some examples are the 19-manganese(II)-containing polyanion Mn^{II}_{19}[7a] and the higher-valent/mixed-valent species $Mn^{III/II}_{16}$,[7b] $Mn^{IV/III}_{10}$,[7c] and Mn^{III}_3.[7d] In particular, the encapsulation of Mn^{3+} (d^4 electron configuration, Jahn−Teller distortion) ions in POMs is attractive due to likely single molecule magnetic (SMM) behavior as well as promising catalytic properties.[8] Interesting examples of POM-based SMMs are the mixed-valence manganese(III/IV)-containing polyanion $[Mn^{III}_4Mn^{II}_2O_4(H_2O)_4(XW_9O_{34})_2]^{12-}$ (X = Si, Ge) with an effective energy barrier of 14.8 K,[8c] as well as the polyanion $[Mn^{III}_3Mn^{IV}O_3(CH_3COO)_3(P_2W_{15}O_{56})]^{8-}$ with a high-spin ground state ($S = 21/2$).[8d] An example for the latter is the mixed-valent tetra-manganese(III/IV)-containing 9-tungstosilicate $[Mn^{III}_3Mn^{IV}O_3(CH_3CO_2)_3(SiW_9O_{34})]^{6-}$ which resembles the active site of photosystem II and indeed displays photocatalytic water oxidation.[8g] It was also shown that the dimanganese(III)-containing Dawson-like polyanion $[Mn^{III}_2W_{17}O_{59}Cl_2]^{12-}$ catalyzed the hydrogen evolution reaction.[8h]

In our continuous effort to prepare multinuclear, high-valent POMs, we decided to investigate the reactivity of the well-

Received: April 25, 2020
Published: August 21, 2020

https://dx.doi.org/10.1021/acs.inorgchem.0c01231
Inorg. Chem. 2020, 59, 13034−13041

known Mn_{12}-acetato complex $[Mn^{III}_8Mn^{IV}_4O_{12}(CH_3COO)_{16}(H_2O)_4]$ (Mn_{12}) with the trilacunary Wells-Dawson-type heteropolytungstate $[P_2W_{15}O_{56}]^{12-}$ in some detail.

2. EXPERIMENTAL SECTION

2.1. Reagents and Instrumentation. The POM precursor salt $Na_{12}[P_2W_{15}O_{56}]\cdot 18H_2O$[9a] and the manganese-12 complex $[Mn^{III}_8Mn^{IV}_4O_{12}(CH_3COO)_{16}(H_2O)_4]\cdot 2CH_3COOH\cdot 4H_2O$[9b] were prepared according to the published procedures and characterized by FT-IR spectroscopy. All other reagents were used as purchased without further purification. The FT-IR spectra were recorded as KBr pellets on a Nicolet Avatar 370 spectrophotometer operating between 400 and 4000 cm^{-1}. Thermogravimetric analysis was carried out on a TA Instruments SDT Q600 thermobalance with flow of nitrogen; the temperature was ramped from room temperature to 800 °C at a rate of 5 °C/min. The ^{31}P NMR spectrum was recorded on a 400 MHz JEOL ECS 400 instrument at room temperature using a 5 mm tube with a resonance frequency of 162.14 MHz and the chemical shift is reported with respect to 85% H_3PO_4 as reference. Elemental analysis for **1a** was performed by Technische Universität Hamburg, Zentrallabor Chemische Analytik, Hamburg, Germany.

Synthesis of $Na_{12}[Mn^{III}_4(H_2O)_2(P_2W_{15}O_{56})_2]\cdot 84H_2O$ (1a). $[Mn^{III}_8Mn^{IV}_4O_{12}(CH_3COO)_{16}(H_2O)_4]\cdot 2CH_3COOH\cdot 4H_2O$ (0.270 g, 0.128 mmol) was suspended in a mixture of 36 mL of CH_3CO_2H and 24 mL of H_2O (resulting in pH 1.1) for 1 h. To this solution, $Na_{12}[P_2W_{15}O_{56}]\cdot 18H_2O$ (1.104 g, 0.256 mmol) was added. After stirring for 30 min at room temperature, the mixture was heated to 80 °C for another 1 h and filtered. Then, NaCl (0.40 g, 6.87 mmol) was added to the solution. The filtrate was kept for crystallization at room temperature. Brown crystals were obtained after a few days. Yield: 0.28 g (22% based on W). Anal. Calcd for $H_{172}Na_{12}Mn_4P_4W_{30}O_{198}$: W, 58.20, Mn, 2.32, P, 1.31, Na, 2.91. Found: W, 57.90; Mn, 1.96; P, 1.23; Na, 3.22. IR ($\tilde{\nu}$/cm^{-1}): 3456(br), 2923(w), 2853(w), 1740(sh), 1616(s), 1455(sh), 1384(w), 1087(s), 1056(w), 944(s), 919(w), 822(sh), 746(br), 680(sh), 515(w).

X-ray Crystallography. A single-crystal of **1a** was mounted on a Hampton cryoloop in light oil for data collection at 100 K on a Bruker D8 SMART APEX II CCD diffractometer with kappa geometry and graphite-monochromated Mo Kα radiation (λ = 0.71073 Å). Data collection, structure solution, and refinement were performed using the *SMART*, *SAINT*, and *SHELXTL* programs, respectively.[10a−e] Multiscan absorption corrections were performed using *SADABS*.[10b] Direct methods (*SHELXS97*) successfully located the tungsten atoms, and successive Fourier syntheses (*SHELXL2014*) revealed the remaining atoms.[10c] Refinements were full-matrix least-squares against $|F^2|$ using all data. All nondisordered heavy atoms (W, Mn, Na, P) were refined anisotropically, whereas oxygen atoms were refined isotropically. No hydrogen atoms were included in the models. The formula unit shown in the CIF file is based on elemental analysis and TGA measurements, as it reflects the true bulk composition of **1a**. The crystallographic parameters for **1a** are given in Table 1. Further details on the crystal structure investigations may be obtained free of charge under CCDC-1905841 from The Cambridge Crystallographic Data Centre via http://www.ccdc.cam.ac.uk/data_request/cif.

XPS Measurements. A 50-nm-thick Au layer was sputter-coated on a silicon substrate to avoid charging during the XPS measurements. Then, **1a** was dispersed in acetone and deposited on the prepared substrate by drop casting. Afterward, the sample was heated at 50 °C for 15 min to evaporate the solvent. After preparation, the sample was introduced into the XPS vacuum vessel. Photoelectrons were excited by a Mg/Al X-ray gun (Specs XP-50) with an incident angle of 45°. For all measurements Mg $K_{\alpha 1,2}$ radiation (E = 1253.6 eV) was used. The analyzer was operated in fixed analyzer transmission mode with a pass energy of 30 eV. The energetic shift in binding energy positions due to charging of the samples was referenced to the C 1s peak. The analysis of the measured data was done with the CASAXPS software. Shirley's method was used to subtract the background. The Mn 2p doublet was fitted using a simplified Voigt function. The intensity ratio was fixed at 0.5 between Mn $2p_{1/2}$ and Mn $2p_{3/2}$. As a reference containing Mn^{III} ions, $Mn(CH_3COO)_3$ was measured for comparison.

Table 1. Crystal Data and Structure Refinement Parameters for 1a

empirical formula	$H_{172}Mn_4Na_{12}O_{198}P_4W_{30}$
formula weight, g/mol	9476.39
temperature (K)	100(2)
crystal system	triclinic
space group	$P\bar{1}$
a (Å)	12.6385(7)
B (Å)	15.7346(8)
C (Å)	19.4554(10)
α (deg)	87.043(2)
β (deg)	84.088(2)
γ (deg)	74.994(2)
volume (Å^3); Z	3715.9(3); 1
density (Mgm^{-3})	4.235
abs. coeff. (mm^{-1})	23.673
F(000)	4268
θ range (deg)	3.4 to 25.242
limiting indices	$-15 \le h \le 16$
	$-16 \le k \le 20$
	$-25 \le l \le 25$
reflections collected	129922
unique reflections [R_{int}]	18391 [0.0467]
completeness to θ	99.7
data/restraints/parameters	18391/0/571
GOF on F^2	1.005
final R indices [$I > 2\sigma(I)$][a]	R_1 = 0.0380, wR_2 = 0.0968
R indices (all data)[b]	R_1 = 0.0467, wR_2 = 0.1021

[a] $R_1 = \sum||F_o| - |F_c||/\sum|F_o|$. [b] $wR_2 = [\sum w(F_o^2 - F_c^2)^2/\sum w(F_o^2)^2]^{1/2}$.

Electrochemical Measurements. All electrochemical experiments were performed with a CHI-660c electrochemical workstation (USA) with a conventional three-electrode electrochemical cell. A glassy carbon electrode (GCE; d = 3 mm, A = 0.0707 cm^{-2}) was used as the working electrode, a platinum wire as the auxiliary/counter electrode (length = 5 cm, d = 0.5 mm), and Ag/AgCl (3 M KCl, E = 0.223 V ± 0.13 mV at 25 °C vs SHE) as the reference electrode. The GCE was polished with 1.0, 0.3, and 0.05 μm Al_2O_3 powders, respectively, and sonicated after each polishing step. Finally, the electrode was washed with ethanol and then dried with a high purity nitrogen stream before use.

Magnetic Susceptibility Measurements. Magnetic susceptibility (χ) measurements were carried out using a Quantum Design MPMS-XL SQUID magnetometer. Data for 24.23 mg of polycrystalline sample **1a** were collected over 1.8−300 K with an applied field of 100 Oe. Previous sample holder measurements were made under identical conditions, and the magnetic response directly subtracted from the raw data. The intrinsic diamagnetic response of the sample was then calculated using Pascal's constants and subtracted from the measured susceptibility.[16] Samples were stored and packed in an argon glovebox prior to measurements.

RESULTS AND DISCUSSION

Synthesis and Structure. We have synthesized and structurally characterized the tetra-Mn^{III}-containing $[Mn^{III}_4(H_2O)_2(P_2W_{15}O_{56})_2]^{12-}$ (**1**), which was prepared by reaction of the mixed-valent Mn_{12}-acetato complex $[Mn^{III}_8Mn^{IV}_4O_{12}(CH_3COO)_{16}(H_2O)_4]$ with the trilacunary Wells-Dawson-type heteropolytungstate $[P_2W_{15}O_{56}]^{12-}$ in acidic acetate solution (pH 1.1). Single-crystal XRD on the

https://dx.doi.org/10.1021/acs.inorgchem.0c01231
Inorg. Chem. 2020, 59, 13034−13041

hydrated sodium salt $Na_{12}[Mn^{III}_4(H_2O)_2(P_2W_{15}O_{56})_2]\cdot 84H_2O$ (**1a**) revealed that four Mn^{III} ions are sandwiched by two $[P_2W_{15}O_{56}]^{12-}$ units leading to the so-called Weakley dimer structure with C_{2h} point group symmetry (Figure 1). The salt

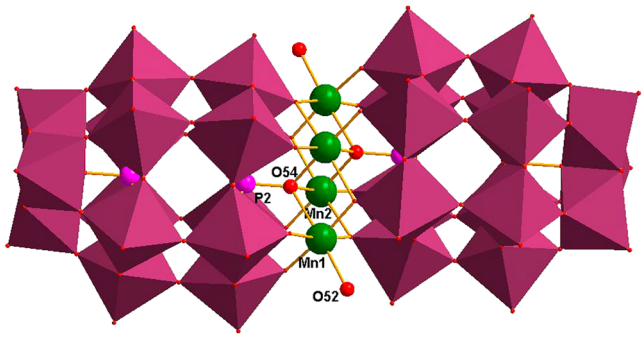

Figure 1. Combined polyhedral/ball-and-stick representation of polyanion **1**.

1a crystallized in the triclinic system with space group $P\bar{1}$, half of polyanion **1** being present in the asymmetric unit. The crystallographic parameters for **1a** are presented in Table 1. The most important IR peaks for polyanion **1** are at 1087 cm^{-1} (P−O bonds), 944 and 822 cm^{-1} (terminal W−O bonds), and 746 cm^{-1} (bridging W−O(W) bonds). The broad peak at 3456 cm^{-1} and the strong peak at 1616 cm^{-1} are attributed to lattice water molecules.

The first example of a M_4-containing sandwich-type POM based on trilacunary Wells-Dawson units was $[M^{II}_4(H_2O)_2(P_2W_{15}O_{56})_2]^{16-}$ (M = Cu, Zn), reported by Weakley and Finke in 1990.[11] In 1994, Coronado's group reported the manganese(II) and nickel(II) derivatives $[M^{II}_4(H_2O)_2(P_2W_{15}O_{56})_2]^{16-}$ (M = Mn, Ni).[12] Hill's group reported the iron(III) derivative of this structure-type, $[Fe^{III}_4(H_2O)_2(P_2W_{15}O_{56})_2)]^{12-}$.[13] On the other hand, to date no Mn^{III}-containing Wells-Dawson sandwich structures have been reported in the literature. The presence of Mn^{III} in **1** was suggested by bond valence sum (BVS) calculations: Mn1, 3.2206; Mn2, 2.6086,[14] as well as the coordination geometry around Mn and the Mn−O bond lengths (Figure 2). The

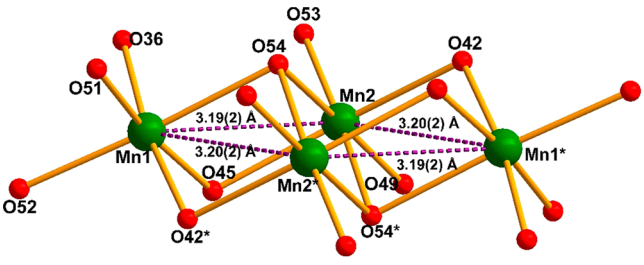

Figure 2. Detailed view of the Mn_4O_{16} core for **1** with atom labeling and Mn···Mn distances.

Mn^{III}−O bond lengths for **1** are shown in Table 2, as well as those of the all-Mn^{II} analogue $[Mn^{II}_4(H_2O)_2(P_2W_{15}O_{56})_2]^{16-}$ (see also Figures S1 and S2).[12] As expected, the higher the oxidation state of manganese, the shorter the Mn−O bonds. Furthermore, the Mn^{III} ions in **1** have a d^4 electronic configuration in an octahedral ligand field (high-spin), which should result in a pronounced Jahn−Teller distortion. In fact, this is exactly what is observed (Figures S1 and S2). A careful evaluation of the Mn1−O and Mn2−O bond lengths in **1** indicates two long axial bonds ($Mn1-O_{axial}$: 2.18(7), 2.31(7) Å; $Mn2-O_{axial}$: 2.21(7), 2.22(7) Å) and four short equatorial bonds ($Mn1-O_{equatorial}$: 1.89−1.91(7) Å; $Mn2-O_{equatorial}$: 1.91−2.12(8) Å) for each manganese(III) ion (see Table 2 for details). Interestingly, in 2012, Wang's group reported the mixed-valence derivative $[Mn^{III}_2Mn^{II}_2(H_2O)_2(P_2W_{15}O_{56})_2]^{14-}$,[15a] which was synthesized by reaction of $Mn(CH_3COO)_2$ with $[P_2W_{15}O_{56}]^{12-}$ and $K_2S_2O_8$ as an oxidant. The two Mn^{III} ions occupy the inner positions of the Mn_4O_{16} rhombus, whereas the two Mn^{II} ions are in the outer positions (Figures S1 and S2). The ^{31}P NMR spectrum of **1a** dissolved in a 60/40 vol % acetic acid/water mixture (pH 1.1) resulted in a singlet at −12.0 ppm (half-width $\Delta\nu_{1/2}$ ca 160 Hz, see Figure S5), which we attribute to the two P atoms distant from the magnetic core of the polyanion.[15b] Presumably the relaxation time of the other two P atoms is very short due to the proximity of the magnetic Mn^{III} ions and hence the NMR signal is wiped out.

X-ray Photoelectron Spectroscopy (XPS) Studies. The oxidation states of the manganese ions in **1** were further confirmed by X-ray photoelectron spectroscopy (XPS) on drop-casted **1a** and manganese(III) acetate ($Mn(CH_3COO)_3$) as a reference. Figure 3 shows the measured XPS spectra and fits for the Mn 2p doublets. The spectrum of **1a** shows binding energies of 642.1 and 653.9 eV for Mn 2p3/2 and Mn 2p1/2, respectively, and for Au 4p1/2 a binding energy of 646.5 eV. The spectrum of manganese(III) acetate shows an essentially identical Mn 2p doublet at binding energies of 642 and 653.8 eV for Mn 2p3/2 and Mn 2p1/2, respectively, with a negligible shift of only 0.1 eV. The weak Au 4p peak is from the underlying substrate. By comparing the binding energies of **1** and Mn^{III} acetate, it can be concluded that the oxidation state of manganese in polyanion **1** is +3, fully consistent with bond valence sum calculations (BVS).[14]

Magnetic Studies. Variable temperature magnetic susceptibility (χ) measurements on polycrystalline **1a** showed that there was no difference between the zero-field cooled (ZFC) and field cooled (FC) measurements, indicating that the sample exhibits no long-range ordering or glassy behavior. Structurally, polyanion **1** contains a well-isolated magnetic M_4 unit with a rhombic spin topology, as displayed in Figures 1 and 2; the rhombohedral symmetry of the M_4 unit simplifies the general spin Hamiltonian to eq 1, which requires only three isotropic spin interactions to account for χ of the Mn_4O_{16} core. Here, the interactions J_a, J_b, and J_c, respectively, correspond to the isotropic interactions between the $S = 2$ Mn^{III} spin centers, i.e., $Mn_1\cdots Mn_2$, $Mn_1\cdots Mn_3$, and $Mn_2\cdots Mn_4$ (Figure 4). Finding of the eigenstates was further simplified by applying the Kambe coupling scheme.[17] In this particular application, pairwise couplings of two spin centers are assumed, i.e., $S_{13} = S_1 + S_3$ and $S_{24} = S_2 + S_4$, with each of these states varying integrally from 0 to 4. In turn, S_{13} and S_{24} are coupled to form a total spin S_T with integral quantum numbers from 0 to 8. The intermediate spin operators allow one to conveniently form an orthogonal basis set that diagonalizes the Hamiltonian, leading to eq 2. The well-known Van Vleck equation was then applied to the resulting energy states to be used in eq 4.[18] The symbols have their standard meaning, where N is Avogadro's number, k the Boltzmann constant, g the Landé g factor, β the Bohr magneton, and ρ the mole fraction of paramagnetic impurity. It should be noted that phenomena such as temperature independent magnetism and axial zero field splitting were

https://dx.doi.org/10.1021/acs.inorgchem.0c01231
Inorg. Chem. 2020, 59, 13034−13041

Table 2. Selected Mn−O Bond Lengths and Mn···Mn Distances (Å) for 1, the Mn^{II}-Containing Analogue $[Mn^{II}_4(H_2O)_2(P_2W_{15}O_{56})_2]^{16-}$,[12] and the Mixed-Valent Derivative $[Mn^{III}_2Mn^{II}_2(H_2O)_2(P_2W_{15}O_{56})_2]^{14-}$ [15a] (see Figure 2 for atom labelling)

bond	1	$[Mn^{II}_4(H_2O)_2(P_2W_{15}O_{56})_2]^{16-}$	$[Mn^{III}_2Mn^{II}_2(H_2O)_2(P_2W_{15}O_{56})_2]^{14-}$	
Mn1−O51(W=O)	1.89(7)	2.08(2)	2.09[b]	Mn^{II}
Mn1−O36(W=O)	1.90(7)	2.11(2)	2.09	
Mn1−O45(μ_2-W=O)	1.91(7)	2.17(2)	2.14	
Mn1−O42(μ_2-W=O)	1.91(7)	2.16(2)	2.17	
Mn1−$O52_{water}$	2.18(7)	2.23(2)	2.17	
Mn1−O54(μ_3−P−O)	2.31(7)	2.22(2)	2.27	
Mn2−O49(W=O)	1.91(8)	2.04(2)	2.01	Mn^{III}
Mn2−O53(W=O)	1.93(8)	2.13(2)	2.00	
Mn2−O54(μ_3−P−O)	2.10(7)	2.23(2)	2.17	
Mn2−O54[a](μ_3−P−O)	2.12(7)	2.26(2)	2.23	
Mn2−O42(μ_2-W=O)	2.21(7)	2.13(2)	1.99	
Mn2−O45(μ_2-W=O)	2.22(7)	2.15(2)	1.98	
Mn1···Mn2	3.19(2)	3.28(6)	3.30	
Mn2···Mn1[a]	3.20(2)	3.29(2)	3.26	
Mn1···Mn1[a]	5.52(2)	5.65(2)	5.68	
Mn2···Mn2[a]	3.23(2)	3.35(2)	3.30	

[a]Symmetry-generated equivalent atom. [b]Due to a problem with the cif file, no esd's could be extracted for this compound.[15a]

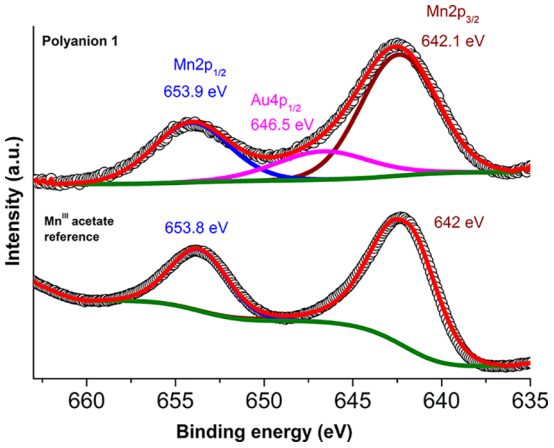

Figure 3. Photoelectron spectra of polyanion **1**.

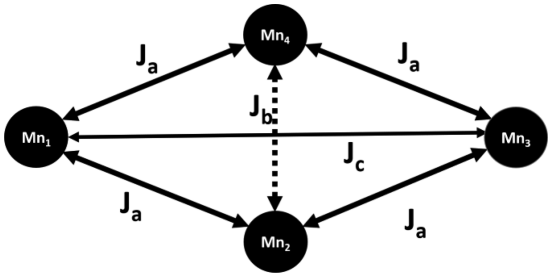

Figure 4. Magnetic coupling scheme for **1**.

not considered, as one would risk an overparameterization. Additionally, J_c could be neglected due to the relatively large distance between the manganese centers and the absence of an oxygen atom to mediate the exchange.

$$\hat{\mathbf{H}} = -2J_a(S_1\cdot S_2 + S_2\cdot S_3 + S_3\cdot S_4 + S_4\cdot S_1) - 2J_b(S_2\cdot S_4) - 2J_c(S_1\cdot S_3) \quad (1)$$

$$E(S_T) = -2J_aS_T(S_T+1) - S_{13}(S_{13}+1)(J_c - J_a) - S_{24}(S_{24}+1)(J_b - J_a) + 12J_b + 12J_c \quad (2)$$

$$\chi = \frac{Ng^2\beta^2}{3kT}\left[(1-\rho)\cdot\frac{A}{B} + S(S+1)\cdot\rho\right] \quad (3)$$

$$A = \sum S_T(S_T+1)(2S_T+1)\, e^{-E(S_T/kT)} \quad (4)$$

$$B = \sum (2S_T+1)\, e^{-E(S_T/kT)} \quad (5)$$

A satisfying description of the experimental data over the whole temperature range was obtained (Figure 5, equation in Supporting Information) with the following set of parameters: $J_a = -2.16 \pm 0.08$ K, $J_b = 3.24 \pm 1.73$ K, $g = 2.35 \pm 0.040$, and $\rho = 0.34 \pm 0.03$. The negative J_a value supports the idea that it

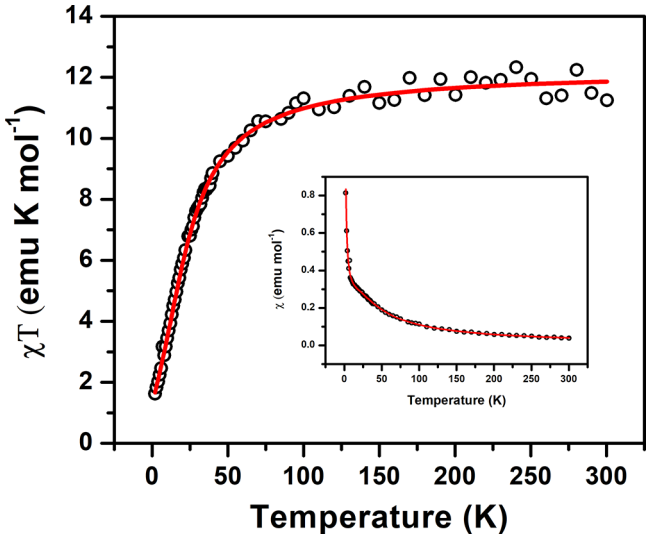

Figure 5. Fit of χT to the temperature dependence of **1a**. The dots are the experimental data, and the solid line represents the best least-squares-fit according to eqs 1−5. The inset shows the same fit applied to χ.

https://dx.doi.org/10.1021/acs.inorgchem.0c01231
Inorg. Chem. 2020, 59, 13034−13041

is the dominant antiferromagnetic spin exchange interaction between the four Mn^{III} ions in **1**, with the positive J_b being a concomitant result. The overall dominant antiferromagnetic character of **1** is clearly reflected in the experimental data for χT. Overall, our present study provides the susceptibility of tetra-guest metal ion-containing heteropolytungstates and extract fitting parameters, which was a limitation in some of the previous studies.[19,20]

Electrochemical Study. The solution redox properties of polyanion **1** were studied by cyclic voltammetry (CV) in a pH 3 buffer (0.1 M Na_2SO_4 + H_2SO_4) on a glassy carbon electrode at a scan rate of 10 mVs^{-1} using Ag/AgCl as a reference electrode. By describing the tungsten-oxo redox behavior of **1**, a set of well-defined four reversible tungsten-oxo redox couples was observed, originating from the trilacunary $\{P_2W_{15}O_{56}\}$ Dawson units in **1**, see the restricted CV shown in Figure 6a.

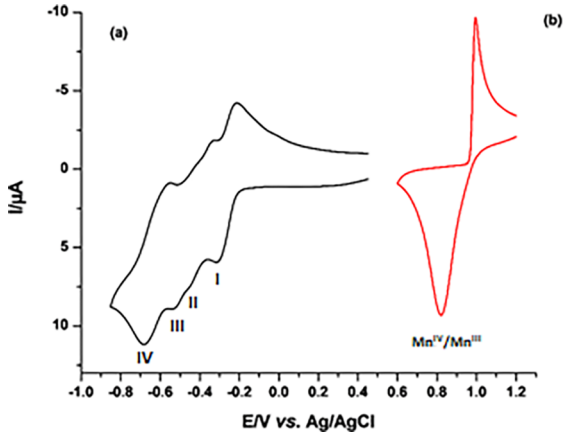

Figure 6. Cyclic voltammograms (CVs) of a solution of 1 mM **1** in pH 3 buffer (0.1 M Na_2SO_4 + H_2SO_4). (a) Redox domain restricted to the tungsten-oxo units in **1**. (b) Redox domain restricted to the Mn^{IV}/Mn^{III} domain in **1**. Glassy carbon working electrode (A = 0.0707 cm^2) vs Ag/AgCl reference electrode.

The redox couples labeled as I and IV ($E_{1/2}$ = −264 mV and −618 mV, respectively) represent two pH-dependent bielectronic redox processes, whereas the redox couples II and III ($E_{1/2}$ = −393 mV and 472 mV, respectively) exhibit monoelectronic processes as shown in eqs 6 to 9, respectively.[15b,21−23]

$$[P_2W_{15}O_{56}]^{12-} + 2e^- + 2H^+ \leftrightarrow [H_2P_2W_{15}O_{56}]^{12-} \quad (6)$$

$$[H_2P_2W_{15}O_{56}]^{12-} + 1e^- + 1H^+ \leftrightarrow [H_3P_2W_{15}O_{56}]^{12-} \quad (7)$$

$$[H_3P_2W_{15}O_{56}]^{12-} + 1e^- + 1H^+ \leftrightarrow [H_4P_2W_{15}O_{65}]^{12-} \quad (8)$$

$$[H_4P_2W_{15}O_{56}]^{12-} + 2e^- + 2H^+ \leftrightarrow [H_6P_2W_{15}O_{56}]^{12-} \quad (9)$$

Figure 6b represents the CV of **1** restricted to the manganese(III)-oxo unit in a pH 3 buffer (0.1 M Na_2SO_4 + H_2SO_4). The reversible redox couple Mn^{IV}/Mn^{III} appears in the potential region of +0.80 V to +1.1 V with $E_{1/2}$ = 0.907 V.[21,22] For comparison, Figure 7 shows the CV of **1** at pH 1 (0.1 M HCl) and 3 (0.1 M Na_2SO_4 + H_2SO_4) using a scan rate of 100 mV/s^{-1}, restricted to the tungsten-oxo redox couples. The CV pattern shows the typical pH-dependent behavior of POMs as the potentials of the tungsten-oxo redox couples move toward more negative values with increasing pH.[24,25]

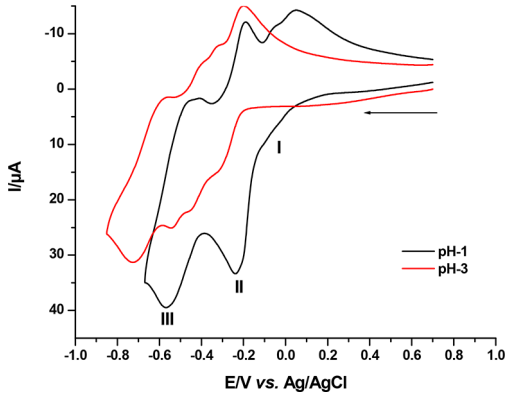

Figure 7. CVs of 1 mM **1** at pH 1 (0.1 M HCl) and 3 (0.1 M Na_2SO_4 + H_2SO_4) with a scan rate of 100 mVs^{-1} using a glassy carbon working electrode (A = 0.0707 cm^2) vs Ag/AgCl reference electrode.

At pH 1 (0.1 M HCl), the reduction waves I and II seem to be largely merged, showing a sharp peak at −0.215 V with a pronounced shoulder at −0.04 V, whereas the reoxidation couple is split in two monoelectronic waves. On the other hand, the bielectronic redox couple III is nicely reversible with $E_{1/2}$ = −500 mV. A scan rate study of **1** in a pH 3 buffer (0.1 M Na_2SO_4 + H_2SO_4) as shown in Figure 8 demonstrates that the

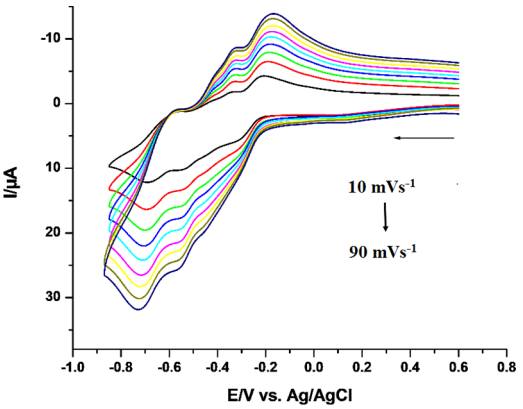

Figure 8. CV of **1** in pH 3 buffer (0.1 M Na_2SO_4 + H_2SO_4) by using a GCE (A = 0.0707 cm^2) as a working electrode vs Ag/AgCl at a scan rate from 10 to 90 mVs^{-1} (from inner to outer curve).

peak currents associated with the tungsten-oxo redox processes increase with increasing scan rate, with the resulting peak currents being proportional to the square root of the scan rate, thereby indicating the diffusion-controlled nature of the redox processes.

CONCLUSIONS

We have synthesized and structurally characterized the tetra-Mn^{III}-containing 30-tungsto-4-phosphate $[Mn^{III}_4(H_2O)_2(P_2W_{15}O_{56})_2]^{12-}$ (**1**) using a simple one-pot synthetic reaction of the mixed-valent Mn_{12} complex $[Mn^{III}_8Mn^{IV}_4O_{12}(CH_3COO)_{16}(H_2O)_4]$ with the trilacunary Wells-Dawson-type heteropolytungstate $[P_2W_{15}O_{56}]^{12-}$ in aqueous acetate solution (pH 1.1). Polyanion **1** has a Weakley-type sandwich structure with a rhombic $Mn^{III}_4O_{16}$ core. Magnetic studies over 1.8−300 K with an applied magnetic field of 100 Oe showed that the intramolecular coupling between the four Mn^{III} ions is primarily of an antiferromagnetic nature, most strongly influenced by the

https://dx.doi.org/10.1021/acs.inorgchem.0c01231
Inorg. Chem. 2020, 59, 13034−13041

negative J_a value, with little evidence for any sharp transitions or spin glass behavior. Electrochemical studies for **1** revealed a reversible Mn^{IV}/Mn^{III} redox couple in the +0.80 to +1.1 V potential region with $E_{1/2}$ = +0.907 V. We are currently in the process of trying to isolate other high-valent and mixed-valent manganese-containing POMs.

■ ASSOCIATED CONTENT

Supporting Information

The Supporting Information is available free of charge at https://pubs.acs.org/doi/10.1021/acs.inorgchem.0c01231.

Detailed view of the coordination chemistry of the manganese ions in **1** and two isostructural analogues (Figures S1 and S2), FTIR spectrum (Figure S3) and thermogram (Figure S4) of **1a**, ^{31}P NMR spectrum of **1a** in D_2O (Figure S5), as well as the equation for the magnetic susceptibility fitting (PDF)

Accession Codes

CCDC 1905841 contains the supplementary crystallographic data for this paper. These data can be obtained free of charge via www.ccdc.cam.ac.uk/data_request/cif, or by emailing data_request@ccdc.cam.ac.uk, or by contacting The Cambridge Crystallographic Data Centre, 12 Union Road, Cambridge CB2 1EZ, UK; fax: +44 1223 336033.

■ AUTHOR INFORMATION

Corresponding Author

Ulrich Kortz − *Department of Life Sciences and Chemistry, Jacobs University, 28759 Bremen, Germany;* orcid.org/0000-0002-5472-3058; Email: u.kortz@jacobs-university.de

Authors

Joydeb Goura − *Department of Life Sciences and Chemistry, Jacobs University, 28759 Bremen, Germany;* orcid.org/0000-0003-2991-3965

Manjiri Choudhari − *Department of Life Sciences and Chemistry, Jacobs University, 28759 Bremen, Germany;* orcid.org/0000-0001-6599-2635

Talha Nisar − *Department of Physics and Earth Sciences, Jacobs University, 28759 Bremen, Germany;* orcid.org/0000-0003-0091-362X

Torsten Balster − *Department of Physics and Earth Sciences, Jacobs University, 28759 Bremen, Germany*

Jasleen K. Bindra − *Department of Chemistry and Biochemistry, Florida State University, Tallahassee, Florida 32306, United States*

Jared Kinyon − *Department of Chemistry and Biochemistry, Florida State University, Tallahassee, Florida 32306, United States*

Bushra Ali − *Dundalk Institute of Technology, Dundalk, County Louth A91 K584, Ireland*

Timothy McCormac − *Dundalk Institute of Technology, Dundalk, County Louth A91 K584, Ireland;* orcid.org/0000-0002-9096-1248

Naresh S. Dalal − *Department of Chemistry and Biochemistry, Florida State University, Tallahassee, Florida 32306, United States;* orcid.org/0000-0002-9996-6918

Veit Wagner − *Department of Physics and Earth Sciences, Jacobs University, 28759 Bremen, Germany;* orcid.org/0000-0002-6831-8600

Complete contact information is available at: https://pubs.acs.org/10.1021/acs.inorgchem.0c01231

Notes

The authors declare no competing financial interest.

■ ACKNOWLEDGMENTS

U.K. thanks the German Research Council (DFG, KO-2288/26-1), Jacobs University, and CMST COST Action CM1203 (PoCheMoN) for support. We thank Mr. Xiang Ma for assistance with NMR and Dr. Bassem S. Bassil for helpful discussions. Figures [1] and [2] were generated with Diamond, version 3.2 (Crystal Impact GbR, Bonn, Germany).

■ REFERENCES

(1) (a) Kostakis, G. E.; Powell, A. K. An approach to describing the topology of polynuclear clusters. *Coord. Chem. Rev.* **2009**, *253*, 2686−2697. (b) Chakraborty, A.; Goura, J.; Kalita, P.; Swain, A.; Rajaraman, G.; Chandrasekhar, V. Heterometallic 3d−4f single molecule magnets containing diamagnetic metal ions. *Dalton Trans.* **2018**, *47*, 8841−8864. (c) Woodruff, D. N.; Winpenny, R. E. P.; Layfield, R. A. Lanthanide single-molecule magnets. *Chem. Rev.* **2013**, *113*, 5110−5148.

(2) (a) Pope, M. T. *Heteropoly and Isopoly Oxometalates*; Springer: Berlin, 1983. (b) Izarova, N. V.; Pope, M. T.; Kortz, U. Noble metals in polyoxometalates. *Angew. Chem., Int. Ed.* **2012**, *51*, 9492−9510.

(3) (a) Ibrahim, M.; Dickman, M. H.; Suchopar, A.; Kortz, U. Large cation− anion materials based on trinuclear Ruthenium (III) salts of Keggin and Wells-Dawson anions having water-filled channels. *Inorg. Chem.* **2009**, *48*, 1649−1654. (b) Bassil, B. S.; Dickman, M. H.; von der Kammer, B.; Kortz, U. The Monolanthanide-Containing Silicotungstates [Ln(β2-SiW11O39)2]13- (Ln = La, Ce, Sm, Eu, Gd, Tb, Yb, Lu): A Synthetic and Structural Investigation. *Inorg. Chem.* **2007**, *46*, 2452−2458. (c) Bartis, J.; Dankova, M.; Lessmann, J. J.; Luo, Q.; Horrocks, W. D.; Francesconi, L. C. Lanthanide Complexes of the α-1 Isomer of the [P2W17O61]10- Heteropolytungstate: Preparation, Stoichiometry, and Structural Characterization by 183W and 31P NMR Spectroscopy and Europium(III) Luminescence Spectroscopy. *Inorg. Chem.* **1999**, *38*, 1042−1053. (d) Haraguchi, N.; Okaue, Y.; Isobe, T.; Matsuda, Y. Stabilization of tetravalent cerium upon coordination of unsaturated heteropolytungstate anions. *Inorg. Chem.* **1994**, *33*, 1015−1020. (e) Kortz, U. Rare-Earth Substituted Polyoxoanions: [{La(CH3COO)(H2O)2(α2-P2W17O61)}2]16− and [{Nd(H2O)3(α2-P2W17O61)}2]14−. *J. Cluster Sci.* **2003**, *14*, 205−214. (f) Bassil, B. S.; Xiang, Y.; Haider, A.; Hurtado, J.; Novitchi, G.; Powell, A. K.; Bossoh, A. M.; Mbomekallé, I. M.; de Oliveira, P.; Kortz, U. Heptanickel (II) double-cubane core in wells-dawson heteropolytungstate,[Ni7(OH)6(H2O)6-(P2W15O56)2]16−. *Chem. Commun.* **2016**, *52*, 2601−2604. (g) Ibrahim, M.; Xiang, Y.; Bassil, B. S.; Lan, Y.; Powell, A. K.; de Oliveira, P.; Keita, B.; Kortz, U. Synthesis, Magnetism, and Electrochemistry of the Ni14- and Ni5-Containing Heteropolytungstates [Ni14(OH)6(H2O)10(HPO4)4(P2W15O56)4]34− and [Ni5(OH)4(H2O)4(β-GeW9O34)(β-GeW8O30(OH))]13−. *Inorg. Chem.* **2013**, *52*, 8399−8408.

(4) (a) Zheng, S.-T.; Yang, G.-Y. Recent advances in paramagnetic-TM-substituted polyoxometalates (TM = Mn, Fe, Co, Ni, Cu). *Chem. Soc. Rev.* **2012**, *41*, 7623−7646. (b) Han, X.-B.; Zhang, Z.-M.; Zhang, T.; Li, Y.-G.; Lin, W.; You, W.; Su, Z.-M.; Wang, E.-B. Polyoxometalate-based cobalt−phosphate molecular catalysts for visible light-driven water oxidation. *J. Am. Chem. Soc.* **2014**, *136*, 5359−5366. (c) Han, X.-B.; Li, Y.-G.; Zhang, Z.-M.; Tan, H.-Q.; Lu, Y.; Wang, E.-B. Polyoxometalate-based nickel clusters as visible light-driven water oxidation catalysts. *J. Am. Chem. Soc.* **2015**, *137*, 5486−5493. (d) Huang, L.; Wang, S.-S.; Zhao, J.-W.; Cheng, L.; Yang, G.-Y. Synergistic Combination of Multi-ZrIV Cations and Lacunary Keggin Germanotungstates Leading to a Gigantic Zr24-Cluster-Substituted Polyoxometalate. *J. Am. Chem. Soc.* **2014**, *136*, 7637−7642. (e) Ibrahim, M.; Haider, A.; Xiang, Y.; Bassil, B. S.; Carey, A. M.; Rullik, L.; Jameson, G. B.; Doungmene, F.; Mbomekallé, I. M.; Oliveira, P. de; Mereacre, V.; Kostakis, G. E.; Powell, A. K.; Kortz, U.

Tetradecanuclear iron (III)-oxo nanoclusters stabilized by trilacunary heteropolyanions. *Inorg. Chem.* **2015**, *54*, 6136−6146 (references therein),. (f) Winter, R. S.; Cameron, J. M.; Cronin, L. Controlling the Minimal Self Assembly of "Complex" Polyoxometalate Clusters. *J. Am. Chem. Soc.* **2014**, *136*, 12753−2761. (g) Godin, B.; Chen, Y.-G.; Vaissermann, J.; Ruhlmann, L.; Verdaguer, M.; Gouzerh, P. Coordination Chemistry of the Hexavacant Tungstophosphate [H2P2W12O48]12− with FeIII Ions: Towards Original Structures of Increasing Size and Complexity. *Angew. Chem., Int. Ed.* **2005**, *44*, 3072−3075. (h) Godin, B.; Vaissermann, J.; Herson, P.; Ruhlmann, L.; Verdaguer, M.; Gouzerh, P. Coordination chemistry of the hexavacant tungstophosphate [H2P2W12O48]12−: synthesis and characterization of iron(iii) complexes derived from the unprecedented {P2W14O54} fragment. *Chem. Commun.* **2005**, 5624−5626. (i) Bassil, B. S.; Nellutla, S.; Kortz, U.; Stowe, A. C.; van Tol, J.; Dalal, N. S.; Keita, B.; Nadjo, L. The Satellite-Shaped Co-15 Polyoxotungstate, [Co6(H2O)30{Co9Cl2(OH)3(H2O)9(β-SiW8O31)3}]5-. *Inorg. Chem.* **2005**, *44*, 2659−2665. (j) Keita, B.; Kortz, U.; Holzle, L. R. B.; Brown, S.; Nadjo, L. Efficient Hydrogen-Evolving Cathodes Based on Proton and Electron Reservoir Behaviors of the Phosphotungstate [H7P8W48O184]33- and the Co(II)-Containing Silicotungstates [Co6(H2O)30{Co9Cl2(OH)3(H2O)9(β-SiW8O31)3}]5- and [{Co3(B-β-SiW9O33(OH))(B-β-SiW8O29OH)2}2]22-. *Langmuir* **2007**, *23*, 9531−9534.

(5) (a) Coronado, E. Molecular magnetism: from chemical design to spin control in molecules, materials and devices. *Nat. Rev. Mater.* **2020**, *5*, 87−104. (b) Coronado, E.; Day, P. Magnetic molecular conductors. *Chem. Rev.* **2004**, *104*, 5419−5448. (c) Clemente-Juan, J. M.; Coronado, E.; Gaita-Ariño, A. Magnetic polyoxometalates: from molecular magnetism to molecular spintronics and quantum computing. *Chem. Soc. Rev.* **2012**, *41*, 7464−7478. (d) Compain, J.-D.; Mialane, P.; Dolbecq, A.; Mbomekallé, I. M.; Marrot, J.; Sécheresse, F.; Riviére, E.; Rogez, G.; Wernsdorfer, W. Iron Polyoxometalate Single-Molecule Magnets. *Angew. Chem., Int. Ed.* **2009**, *48*, 3077−3081. (e) Ibrahim, M.; Mereacre, V.; Leblanc, N.; Wernsdorfer, W.; Anson, C. E.; Powell, A. K. Self-Assembly of a Giant Tetrahedral 3 d−4 f Single-Molecule Magnet within a Polyoxometalate System. *Angew. Chem., Int. Ed.* **2015**, *54*, 15574−15578.

(6) (a) Mal, S. S.; Kortz, U. The Wheel-Shaped Cu20 Tungstophosphate [Cu20Cl(OH)24(H2O)12(P8W48O184)]25− Ion. *Angew. Chem., Int. Ed.* **2005**, *44*, 3777−3780. (b) Mal, S. S.; Dickman, M. H.; Kortz, U.; Todea, A. M.; Merca, A.; Bögge, H.; Glaser, T.; Müller, A.; Nellutla, S.; Kaur, N.; van Tol, J.; Dalal, N. S.; Keita, B.; Nadjo, L. Nucleation Process in the Cavity of a 48-Tungstophosphate Wheel Resulting in a 16-Metal-Centre Iron Oxide Nanocluster. *Chem. - Eur. J.* **2008**, *14*, 1186−1195. (c) Ibrahim, M.; Lan, Y.; Bassil, B. S.; Xiang, Y.; Suchopar, A.; Powell, A. K.; Kortz, U. Hexadecacobalt(II)-Containing Polyoxometalate-Based Single-Molecule Magnet. *Angew. Chem., Int. Ed.* **2011**, *50*, 4708−4711. (d) Ibrahim, M.; Haider, A.; Lan, Y.; Bassil, B. S.; Carey, A. M.; Liu, R.; Zhang, G.; Keita, B.; Li, W.; Kostakis, G. E.; Powell, A. K.; Kortz, U. Multinuclear Cobalt(II)-Containing Heteropolytungstates: Structure, Magnetism, and Electrochemistry. *Inorg. Chem.* **2014**, *53*, 5179−5188. (e) Bassil, B. S.; Dickman, M. H.; Römer, I.; von der Kammer, B.; Kortz, U. The Tungstogermanate [Ce20Ge10W100O376(OH)4(H2O)30]56−: A Polyoxometalate Containing 20 Cerium(III) Atoms. *Angew. Chem., Int. Ed.* **2007**, *46*, 6192−6195. (f) Wang, K.-Y.; Bassil, B. S.; Lin, Z.; Romer, I.; Vanhaecht, S.; Parac-Vogt, T. N.; Saenz de Pipaon, C.; Galan-Mascaros, J. R.; Fan, L.; Cao, J.; Kortz, U. Ln12-Containing 60-Tungstogermanates: Synthesis, Structure, Luminescence, and Magnetic Studies. *Chem. - Eur. J.* **2015**, *21*, 18168−18176.

(7) (a) Bassil, B. S.; Ibrahim, M.; Al-Oweini, R.; Asano, M.; Wang, Z.; van Tol, J.; Dalal, N. S.; Choi, K.-Y.; Ngo Biboum, R.; Keita, B.; Nadjo, L.; Kortz, U. A Planar {Mn19(OH)12}26+ Unit Incorporated in a 60-Tungsto-6-Silicate Polyanion. *Angew. Chem., Int. Ed.* **2011**, *50*, 5961−5964. (b) Haider, A.; Ibrahim, M.; Bassil, B. S.; Carey, A. M.; Viet, A. N.; Xing, X.; Ayass, W. W.; Minambres, J. F.; Liu, R.; Zhang, G.; Keita, B.; Mereacre, V.; Powell, A. K.; Balinski, K.; N'Diaye, A. T.; Kupper, K.; Chen, H.-Y.; Stimming, U.; Kortz, U. Mixed-Valent Mn16-Containing Heteropolyanions: Tuning of Oxidation State and Associated Physicochemical Properties. *Inorg. Chem.* **2016**, *55*, 2755−2764. (c) Al-Oweini, R.; Bassil, B. S.; Itani, M.; Emiroğlu, D. B.; Kortz, U. The mixed-valent 10-manganese (III/IV)-containing 36-tungsto-4-arsenate (V),[MnIII6MnIV4O4(OH)12(H2O)12(A-β-AsW9O34)4] 22−. *Acta Crystallogr., Sect. C: Struct. Chem.* **2018**, *C74*, 1390−1394. (d) Al-Oweini, R.; Bassil, B. S.; Palden, T.; Keita, B.; Lan, Y.; Powell, A. K.; Kortz, U. The manganese(III)-containing tungstophosphate [MnIII3(H2O)5(A-α-PW9O34)2]9−. *Polyhedron* **2013**, *52*, 461−466.

(8) (a) Zhang, X.-Y.; O'Connor, C. J.; Jameson, G. B.; Pope, M. T. High-Valent Manganese in Polyoxotungstates. 3. Dimanganese Complexes of γ-Keggin Anions. *Inorg. Chem.* **1996**, *35*, 30−34. (b) Khenkin, A. M.; Kumar, D.; Shaik, S.; Neumann, R. Characterization of Manganese(V)−Oxo Polyoxometalate Intermediates and Their Properties in Oxygen-Transfer Reactions. *J. Am. Chem. Soc.* **2006**, *128*, 15451−15460. (c) Ritchie, C.; Ferguson, A.; Nojiri, H.; Miras, H. N.; Song, Y.-F.; Long, D.-L.; Burkholder, E.; Murrie, M.; Kögerler, P.; Brechin, E. K.; Cronin, L. Polyoxometalate-Mediated Self-Assembly of Single-Molecule Magnets: {[XW9O34]2-[MnIII4MnII2O4(H2O)4]}12−. *Angew. Chem., Int. Ed.* **2008**, *47*, 5609−5612. (d) Fang, X.; Kögerler, P.; Speldrich, M.; Schilder, H.; Luban, M. A polyoxometalate-based single-molecule magnet with an S = 21/2 ground state. *Chem. Commun.* **2012**, *48*, 1218−1220. (e) Fang, X.; Speldrich, M.; Schilder, H.; Cao, R.; O'Halloran, K. P.; Hill, C. L.; Kögerler, P. Switching slow relaxation in a MnIII3MnIV cluster: an example of grafting single-molecule magnets onto polyoxometalates. *Chem. Commun.* **2010**, *46*, 2760−2762. (f) Zhang, Z.-M.; Yao, S.; Li, Y.-G.; Wu, H.-H.; Wang, Y.-H.; Rouzieres, M.; Clerac, R.; Su, Z.-M.; Wang, E.-B. A polyoxometalate-based single-molecule magnet with a mixed-valent {MnIV2MnIII6MnII4} core. *Chem. Commun.* **2013**, *49*, 2515−2517. (g) Al-Oweini, R.; Sartorel, A.; Bassil, B. S.; Natali, M.; Berardi, S.; Scandola, F.; Kortz, U.; Bonchio, M. Photocatalytic Water Oxidation by a Mixed-Valent MnIII3MnIVO3Manganese Oxo Core that Mimics the Natural Oxygen-Evolving Center. *Angew. Chem., Int. Ed.* **2014**, *53*, 11182−11185. (h) Jiao, Y.-Q.; Qin, C.; Wang, X.-L.; Liu, F.-H.; Huang, P.; Wang, C.-G.; Shao, K.-Z.; Su, Z.-M. Redox-controlled δ-Dawson {Mn2IIIW17} polyoxometalate with photocatalytic H2 evolution activity. *Chem. Commun.* **2014**, *50*, 5961−5963. (i) Sato, R.; Suzuki, K.; Minato, T.; Shinoe, M.; Yamaguchi, K.; Mizuno, N. Field-induced slow magnetic relaxation of octahedrally coordinated mononuclear Fe(III)-, Co(II)-, and Mn(III)-containing polyoxometalates. *Chem. Commun.* **2015**, *51*, 4081−4084. (j) Zhang, C.; Zhang, M.; Shi, H.; Zeng, Q.; Zhang, D.; Zhao, Y.; Wang, Y.; Ma, P.; Wang, J.; Niu, J. A high-nuclearity isopolyoxotungstate based manganese cluster: one-pot synthesis and step-by-step assembly. *Chem. Commun.* **2018**, *54*, 5458−5461.

(9) (a) Finke, R. G.; Droege, M. W.; Domaille, P. J. Trivacant heteropolytungstate derivatives. 3. Rational syntheses, characterization, two-dimensional tungsten-183 NMR, and properties of tungstometallophosphates P2W18M4(H2O)2O6810- and P4W30M4(H2O)2O11216- (M = cobalt, copper, zinc). *Inorg. Chem.* **1987**, *26*, 3886−3896. (b) Lis, T. Preparation, structure, and magnetic properties of a dodecanuclear mixed-valence manganese carboxylate. *Acta Crystallogr., Sect. B: Struct. Crystallogr. Cryst. Chem.* **1980**, *36*, 2042−2046.

(10) (a) *SMART & SAINT Software Reference manuals, Version 6.45*; Bruker Analytical X-ray Systems, Inc.: Madison, WI, 2003. (b) Sheldrick, G. M. *SADABS, a software for empirical absorption correction*, version 2.05; University of Göttingen: Göttingen, Germany, 2002. (c) *SHELXTL Reference Manual*, Ver. 6.c1; Bruker Analytical X-ray Systems, Inc.: Madison, WI, 2000. (d) Sheldrick, G. M. *SHELXTL*, Ver. 6.12; Bruker AXS Inc.: Madison, WI, 2001. (e) Sheldrick, G. M. *SHELXL97, Program for Crystal Structure Refinement*; University of Göttingen: Göttingen, Germany, 1997.

(11) Weakley, T. J. R.; Finke, R. G. Single-crystal x-ray structures of the polyoxotungstate salts K8.3Na1.7[Cu4(H2O)2(PW9O34)2]·

https://dx.doi.org/10.1021/acs.inorgchem.0c01231
Inorg. Chem. 2020, 59, 13034−13041

24H2O and Na14Cu[Cu4(H2O)2(P2W15O56)2]·53H2O. *Inorg. Chem.* **1990**, *29*, 1235−1241.
(12) Gómez-García, C. J.; Borrás-Almenar, J. J.; Coronado, E.; Ouahab, L. Single-Crystal X-ray Structure and Magnetic Properties of the Polyoxotungstate Complexes Na16[M4(H2O)2(P2W15O56)2]·nH2O (M = MnII, n = 53; M = NiII, n = 52): An Antiferromagnetic MnII Tetramer and a Ferromagnetic NiII Tetramer. *Inorg. Chem.* **1994**, *33*, 4016−4022.
(13) Zhang, X.; Chen, Q.; Duncan, D. C.; Lachicotte, R. J.; Hill, C. L. Multiiron Polyoxoanions. Synthesis, Characterization, X-ray Crystal Structure, and Catalytic H2O2-Based Alkene Oxidation by [(n-C4H9)4N]6[FeIII4(H2O)2(PW9O34)2]. *Inorg. Chem.* **1997**, *36*, 4381−4386.
(14) Brown, I. D.; Altermatt, D. Bond-Valence Parameters Obtained from a Systematic Analysis of the Inorganic Crystal Structure Database. *Acta Crystallogr., Sect. B: Struct. Sci.* **1985**, *B41*, 244−247.
(15) (a) Yao, S.; Yan, J.; Yu, Y.; Wang, E. Mixed-valence manganese cluster containing a sandwich-type polyoxometalate. *J. Coord. Chem.* **2012**, *65*, 1451−1458. (b) Ruhlmann, L.; Nadjo, L.; Canny, J.; Contant, R.; Thouvenot, R. Di- and Tetranuclear Dawson-Derived Sandwich Complexes: Synthesis, Spectroscopic Characterization, and Electrochemical Behavior. *Eur. J. Inorg. Chem.* **2002**, *2002*, 975−986.
(16) Bain, G. A.; Berry, J. F. Diamagnetic Corrections and Pascal's Constants. *J. Chem. Educ.* **2008**, *85*, 532.
(17) Kambe, K. J. On the Paramagnetic Susceptibilities of Some Polynuclear Complex Salts. *J. Phys. Soc. Jpn.* **1950**, *5*, 48−51.
(18) van Vleck, J. H. *The Theory of Electric and Magnetic Susceptibilities*; Oxford University Press: Oxford, 1932.
(19) (a) Wang, K. Y.; Bassil, B. S.; Xing, X.; Keita, B.; Bindra, J. K.; Diefenbach, K.; Dalal, N. S.; Kortz, U. Incorporation of Transition-Metal-Ion Guests (Co2+, Ni2+, Cu2+, Zn2+) into the Ti2-Containing 18-Tungsto-2-arsenate(III) Monolacunary Host. *Eur. J. Inorg. Chem.* **2016**, *36*, 5519−5529. (b) Kortz, U.; Jeannin, Y. P.; Tézé, A.; Hervé, G.; Isber, S. A Novel Dimeric Ni-Substituted β-Keggin Silicotungstate: Structure and Magnetic Properties of K12[{β-SiNi2W10O36(OH)2(H2O)}2]·20H2O. *Inorg. Chem.* **1999**, *38*, 3670−3675. (c) Das, L. K.; Biswas, A.; Kinyon, J. S.; Dalal, N. S.; Zhou, H.; Ghosh, A. Di-, Tri-, and Tetranuclear Nickel(II) Complexes with Oximato Bridges: Magnetism and Catecholase-like Activity of Two Tetranuclear Complexes Possessing Rhombic Topology. *Inorg. Chem.* **2013**, *52*, 11744−11757. (d) Bassil, B. S.; Haider, A.; Ibrahim, M.; Mougharbel, A. S.; Bhattacharya, S.; Christian, J. H.; Bindra, J. K.; Dalal, N. S.; Wang, M.; Zhang, G.; Keita, B.; Rutkowska, I. A.; Kulesza, P. J.; Kortz, U. 15-Copper(II)-containing 36-tungsto-4-silicates(IV) [Cu15O2(OH)10X(A-α-SiW9O34)4]25− (X = Cl, Br): synthesis, structure, magnetic properties, and electrocatalytic CO2 reduction. *Dalton Trans.* **2018**, *47*, 12439−12448.
(20) (a) Murray, K. S. The Magnetochemistry of Homo-and Hetero-Tetranuclear First-Row d-Block Complexes. *Adv. Inorg. Chem.* **1995**, *43*, 261−358. (b) Halcrow, M. A.; Sun, J. S.; Huffman, J. C.; Christou, G. Structural and Magnetic Properties of [Ni4(μ3-OMe)4(dbm)4(MeOH)4] and [Ni4(η1,μ3-N3)4(dbm)4(EtOH)4]. Magnetostructural Correlations for [Ni4 × 4]4+ Cubane Complexes. *Inorg. Chem.* **1995**, *34*, 4167−4177. (c) ElFallah, M. S.; Rentschler, E.; Caneschi, A.; Gatteschi, D. Synthesis, crystal structure and magnetic properties of the tetranuclear complex [Ni4(OCH3)4(dbm)4(CH3OH)4]2(C2H5)2O. *Inorg. Chim. Acta* **1996**, *247*, 231−235. (d) Escuer, A.; Font-Bardia, M.; Kumar, S. B.; Solans, X.; Vicente, R. Two new nickel(II) cubane compounds derived from pyridine-2-methoxide (Pym): {Ni4(Pym)4Cl4(CH3OH)4} and {Ni4(Pym)4(N3)4(CH3OH)4}. Crystal structures and magnetic properties. *Polyhedron* **1999**, *18*, 909−914. (e) Mukherjee, S.; Weyhermüller, T.; Bothe, E.; Wieghardt, K.; Chaudhuri, P. Single-Atom O-Bridged Urea in a Dinickel(II) Complex together with NiII4, CuII2 and CuII4 Complexes of a Pentadentate Phenol-Containing Schiff Base with (O,N,O,N,O)-Donor Atoms. *Eur. J. Inorg. Chem.* **2003**, *2003*, 863−875. (f) Clemente-Juan, J. M.; Chansou, B.; Donnadieu, B.; Tuchagues, J. P. Synthesis, Structure, and Magnetic Properties of the Low-Symmetry Tetranuclear Cubane-like Nickel Complex [Ni4(pypentO)(pym)(μ3-OH)2(μ-Oac)2(NCS)2(OH2)]. *Inorg. Chem.* **2000**, *39*, 5515−5519.
(21) Lebrini, M.; Mbomekalle, I. M.; Dolbecq, A.; Marrot, J.; Berthet, P.; Ntienoue, J.; Sécheresse, F.; Vigneron, J.; Etcheberry, A. Manganese(III)-Containing Wells−Dawson Sandwich-Type Polyoxometalates: Comparison with their Manganese(II) Counterparts. *Inorg. Chem.* **2011**, *50*, 6437−6448.
(22) Mbomekalle, I. M.; Keita, B.; Nadjo, L.; Berthet, P.; Neiwert, W. A.; Hill, C. L.; Ritorto, M. D.; Anderson, T. M. Manganous heteropolytungstates. Synthesis and heteroatom effects in Wells−Dawson-derived sandwich complexes. *Dalton Trans.* **2003**, 2646−2650.
(23) Doungmene, F.; Aparicio, P. A.; Ntienoue, J.; Mezui, C. S. A.; de Oliveira, P.; Lopez, X.; Mbomekalle, I. M. Electrochemical behaviour of mixed d metal-iron containing Wells-Dawson sandwich-type complexes: [(FeOH2)2M2(X2W15O56)2]n− and [(MOH2)-2Fe2(X2W15O56)2]n− (M = CrIII, MnIII, MnII, CoII, NiII, CuII, ZnII, X = AsV or PV and n = 12 or 14). *Electrochim. Acta* **2014**, *125*, 674−682.
(24) Ruhlmann, L.; Genet, G. Wells−Dawson-derived tetrameric complexes {K28H8[P2W15Ti3O60.5]4} electrochemical behaviour and electrocatalytic reduction of nitrite and of nitric oxide. *J. Electroanal. Chem.* **2004**, *568*, 315−318.
(25) Wang, C.-L.; Liu, S.-X.; Sun, C.-Y.; Xie, L.-H.; Ren, Y.-H.; Liang, D.-D.; Cheng, H.-Y. Bimetals substituted germanotungstate complexes with open Wells-Dawson structure: Synthesis, structure, and electrochemical behavior of [{M(H2O)}(μ-H2O)2K{M(H2O)-4}(Ge2W18O66)]11− (M = Co, Ni, Mn). *J. Mol. Struct.* **2007**, *841*, 88−95.

https://dx.doi.org/10.1021/acs.inorgchem.0c01231
Inorg. Chem. 2020, 59, 13034−13041